EIGENPROBLEMS FOR SELECTED NANOSTRUCTURES EMBEDDED IN A MATRIX

A. Muc[1], A. Banaś[2]

Institute of Machine Design, Cracow University of Technology, Kraków, Poland
[1] olekmuc@mech.pk.edu.pl, [2] olek.banas@gmail.com

Keywords: Quantum dot; Eigenstates; Numerical Modeling; Wavelets.

Abstract:
In the paper an analytical method of the solution of the governing nonlinear eigenproblem is proposed. It can be directly applied into the analysis of eigenstates in quantum mechanics. The method is based on the use of the separation of variables for specific shapes of quantum dots. In this way the analysis can be reduced to the discretization along one variable only – the Daubechies wavelets or linear finite elements or Fourier series. The eigenstates are derived with the use of the variational formulation combined with the method of the Rayleigh quotient and the series expansions (Bessel functions). The solved two- and three-dimensional examples show the efficiency and the effectiveness of the proposed method. The method can be easily applicable to different physical problems described by the Helmholtz equations.

1. Introduction

Rapid advances in chemical synthesis and fabrication techniques have led to novel nano-sized materials that exhibit unique and often unforeseen properties. One of the greatest advantages of those nanosystems is the ability to control their electronic and optical properties through the sample's size, shape and topology. The design of nanoelectronic devices requires a clear understanding of the fundamental properties of nanomaterials. When nanomaterials absorb a light quantum, two charged particles are created simultaneously, an electron and a hole. Knowledge of photoinduced charge carrier dynamics in nanomaterials will help to achieve an effective functionality of prospective nanonelectronic devices. In recent decades semiconductor quantum dots (QD) have been the subject of many experimental, theoretical and technological investigations.

QDs are tiny dimensionally confined (typically semiconductor) objects where quantum effects become obvious, for example, energy spectra become discrete. Of particular interest is the class of devices that are composed of combinations of lattice mismatched materials. These material combinations, such as Si_xGe_{1-x}/Si and $In_xGa_{1-x}As$/GaAs, where x indicates the fractional content of alloying material, are selected primarily on the basis of their electronic properties and to some extent for convenience of processing. Quantum effects begin to dominate as the size of semiconductor structures approaches the electron de Broglie wavelength. In low-dimensional semiconductor nanostructures (LDSN), the motion of electrons can be confined spatially, from one, two, and even three spatial directions. The operation of semiconductor quantum devices is based on the confinement of individual electrons and holes in one spatial dimension (quantum wells), two spatial dimensions

(quantum wires) or three spatial dimensions (quantum dots - QDs). For instance the potential barriers forming the well are provided primarily by either free surfaces, which impose essentially infinite confinement, or by sharply layered compositional differences. Common configurations of QDs are: cuboidal, conical, lens shaped (ellipsoidal), pyramidal, truncated pyramidal or hemispherical, whereas quantum wires: trapezoidal or cylindrical.

Yet fundamental understanding of the underlying physics responsible for carrier dynamics and the specific role that phonons play in the relaxation mechanisms in QDs is still lacking. In such nanostructures, the free carriers are confined to a small region of space by potential barriers, and if the size of this region is less than the electron wavelength, the electronic states become quantized at discrete energy levels. The ultimate limit of low dimensional structures is the quantum dot, in which the carriers are confined in all three directions. Therefore, a quantum dot can be thought of as an artificial atom.

Many of the previous numerical modeling approaches for these quantum structures used spatial discretisation methods, such as the finite element or finite difference method [1-3]. As an alternative, the boundary element method was proposed by Geldbard, Malloy [4]. Voss [5] employed the Rayleigh-Ritz method to solve the nonlinear eigenvalue problem where the eigenstates of the electron in QDs were derived with the use of the finite element method incorporated in the MATLAB package. Lew Yan Voon, Willatzen [6, 7] found an analytical solutions for paraboloidal and ellipsoidal QDs not embedded in the matrix. Various aspects of the evaluation of the eigenenergies in closed periodic systems of quantum dots were also discussed in the literature - see e.g. Refs [8,9].

Even in devices free of misfit dislocations, the strain induced by lattice mismatch can strongly affect electronic properties. However, this effect has not been thoroughly studied, particularly in submicron sized structures in which quantum mechanics governs the device properties and in which strains are highest and most nonuniform. In order to analyze strain effects in semiconductor quantum structures, it is necessary to adopt a model for electronic properties. Simple quantum mechanical models have long been available for describing the electronic properties of semiconductor devices based on the transport and confinement of single charge carriers. The study of quantum dots and quantum wires has renewed the interest in these models. The effects of uniform, coherent strain on electronic properties have also been well understood for many years and have been identified experimentally by Zaslavsky et al. [10]. There have been some attempts to model strain effects in quantum dots – see e.g. Ref [3]. Further, many quantum dot structures have a well-pronounced piezoelectric effect which does contribute to their overall properties in a non-trivial manner. These coupled elelectromechanical effects will become increasingly important for the current and future applications of such nanostructures – see Refs [11-13].
In the present paper the use of wavelet method/linear finite elements/Fourier series combined with the analytical approach in quantum mechanical nonlinear eigenvalue problem is investigated. The solutions are obtained for 2D and 3D cases of quantum dots embedded in the matrix. Wavelet bases appear to be attractive as a general approach for a wide range of potentials, and not only for quantum dots. In the mathematical sense the problem is described by the solution of the Helmholtz equation.

2. Formulation of the problem

By adopting this continuum view of confinement in semiconductor quantum devices, the spectrum of confined states available to individual electrons or holes can be characterized by the steady state Schrodinger equation, given by:

$$H_i(m_i)\Phi_i = E\Phi_i \text{ where } H_i(m_i) = -div\left(\frac{\hbar^2}{2m_i} grad\Phi_i\right) + V_i(x)\Phi_i,\ x \in \Omega_1 \cup \Omega_2 \qquad (1)$$

where Hi is the Hamiltonian function (operator), Φi is the quantum mechanical wave function associated with energy band, E denotes the energy level (the identical value for the matrix and the quantum dot), ħ is the reduced Planck constant, and the index i corresponds to the quantum dot (i=1; q) and to the matrix (i=2; m), respectively. The solution of the problem depends on boundary conditions; free surfaces impose the physical requirement that Φi =0 for all i. Conditions on boundaries that are remote from regions of interest in the device do not significantly affect energies or wave functions in regions of interest that are solutions to Eq. (1).The steady state Schrődinger (1), which governs the behavior of individual charge carriers in strained devices, is in the form of the classical Helmholtz equation:

$$divgrad\Phi_i + k_i^2\Phi_i = 0,\ k_i^2 = \frac{2m_i(E - V_i)}{\hbar^2},\ i=1,2 \qquad (2)$$

The weak form of the equation (1) is obtained by forming the inner product of each term in the equation with the wave function vector field Φ_i and integrating over the volume of the body. Multiplying (1) by Ψ in the Sobolev space $H_1^0(\Omega), \Omega = \Omega_1 \cup \Omega_2$ and integrating by parts one gets the variational form of the Schrödinger equation:

$$a(\Phi,\Psi;E) = \sum_{i=1}^{2}\int_{\Omega}\left(\frac{\hbar^2}{2m_i} grad\Phi \cdot grad\Psi + V_i(x)\Phi\cdot\Psi\right)d\Omega = E\int\Phi\cdot\Psi d\Omega = Eb(\Phi,\Psi),\ E(\Phi) = \frac{a(\Phi,\Phi;E)}{b(\Phi,\Phi)} \qquad (3), (4)$$

Eq. (1) is the Euler equation which results from the requirement that Eq. (3) must be stationary under variations in Ψ. If the quadratic form $a(\Phi,\Phi;E)$ is a positive, monotonically decreasing function then an unique positive solution exists (4) and the corresponding eigenvectors Φ_k are stationary elements of E'(Φ_k). If the quadratic form *a* does not dependent on *E*, then the above Rayleigh functional is just the well known Rayleigh quotient. The evaluation of the Rayleigh functional is based on the discretization method of the eigenvectors Φ_k. The standard approach is based on the finite element discretization of the body. Some problems can be solved in the analytical way (dependant on the form of QDs) by the separation of variables - see Refs [6,7,14]. Now, we adopt wavelets as general and flexible tool for the solution of time independent Schrodinger (Helmholtz) equation.

3. Separation of variables

It is well-known that for the Helmholtz equation (2) separates in eleven coordinate systems – see Boyer et al. [15]. The separation of variables have been directly used in solving Eq. (2) for the special shapes of quantum dots – see Refs [6,7,14]. One of those situations occurs for the cylindrical coordinates. It is commonly accepted that if the distance of the QD from any free boundary is significantly larger than the QD highest dimension (i.e. three times) then the host matrix boundaries do not impact the solution. Therefore, let us assume that the obtained further solutions are valid in the cylindrical system of coordinates. Using, it the wave function can be written as Eq. (5):

$$\Phi(r,z,\theta) = R(r)Z(z)\Theta(\theta), \qquad \left(\frac{x}{a}\right)^p + \left(\frac{y}{b}\right)^p = 1 \qquad (5),\ (6)$$

A lot of planar curves can be expressed in the form of the superellipse defined as Eq. (6). where *a*, *b* and *p* are positive rational numbers. A supercircle will obviously correspond to setting *a* = *b*. For each value of *p* – the supercircular exponent – we obtain a different curve. The shapes of the supercircles for different values of *n* are shown in Fig. 1. Evidently, *p* = 2 corresponds to a circle whereas *p*= 1 corresponds to a square with its sides rotated by an angle of $\pi/4$. The case $p \to \infty$ also corresponds to a square with its sides parallel to the axes. Finally, the curve Γ characterizing the supercircle can be represented in the form of the Fourier series:

$$\Gamma: \quad \sum_{n=0}^{\infty} G_n \cos(4n\theta) \text{ for the constant } z \text{ value} \tag{7}$$

The above relation exploits the symmetry with respect to the OX and OY axes.

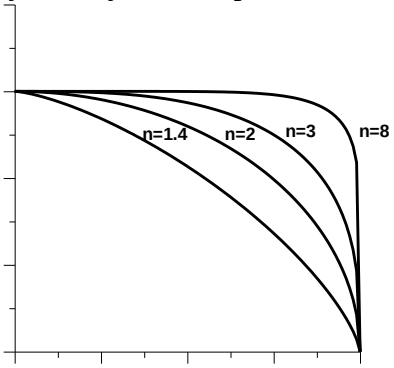

Figure.1 Shape of the supercircle for different values of p

Inserting the relations (5) and (7) into the Helmholtz equation (2) we obtain the following form:

$$\left(\frac{1}{r}\frac{\partial}{\partial r}\left(r\frac{\partial}{\partial r}\right)+k_i^2+s_i^2-\frac{(4n)^2}{r^2}\right)R_i(r)=0\,,\ \frac{\partial^2 Z_i(z)}{\partial z^2}+s_i^2 Z_i(z)=0\,,\ \text{i=1,2} \tag{8}$$

and s_i are the separation constants. If we rescale the spatial coordinate r in Eq. (8) and introduce a new variable $x=r\sqrt{k_i^2+s_i^2}$, the first equation can be reduced to the classical form of the Bessel equation:

$$\left(\frac{1}{x}\frac{\partial}{\partial x}\left(x\frac{\partial}{\partial x}\right)+1-\frac{(4n)^2}{x^2}\right)X_i(x)=0, X_i(x)=R_i(r) \tag{9}$$

Since the Bessel function $J_{-4n}(x)$ tends to an infinity at x=0, the solutions of the above equation exist for the nonnegative values of the natural numbers n. The solution of the equations (9) can be represented in the form of the Bessel function so that we propose to define the radial part of the eigenvectors in the form of the orthogonal Bessel functions:

$$R(r)=\sum_{m=1}^{\infty} A_m^{(4n)} J_{4n}\left(\frac{\mu_m^{(4n)}}{r_0}r\right),\ Z(z)=\sum_{l=0}^{\infty} C_l \sin\left(\frac{l\pi(z-z_0)}{z_1-z_0}\right),\ Z(z)=\sum_{l=1}^{all\,nodes} C_l N_l \tag{10), (11), (12}$$

where the symbols $\mu_m^{(4n)}$ denote the m-th zero of the Bessel function J_{4n} at $r=r_0$. Let us note that each constant $A_m^{(4n)}$ is parameterized also by the value *n*.

In the z direction the expansion of the function Z(z) in the classical Fourier series seems to be the simplest form of its representation, i.e: (11) where z_1 and z_0 denotes the upper and lower boundaries of the quantum dot, respectively.
The next approach is associated with the use of the one dimensional finite elements, i.e. the function Z(z) is expressed in terms of nodal values and element shape functions, as: (12).
The representation of a trial wavefunction as a linear combination of finite elements was discussed by Strang [15].
The last possibility, considered herein, is connected with the use of the wavelet method. Over the last couple of decades, wavelets in general have gained a respectable status due to their applications in various disciplines and as such have many success stories. Notable impacts of their studies are in the fields of signal and image processing, numerical analysis, differential and integral equations, tomography, etc. Wavelets have the ability to represent functions at different levels of resolution, which allows developing a hierarchy of approximate solutions of equations. Compactly supported wavelets are localized in space, wherein solutions can be refined in regions of sharp variations/transients without going for new grid generation, which is the common strategy in classical numerical schemes. Particularly interesting from the point of view of electronic structure calculations is the work by Cho et al. [16], exploring the use of the "Mexican hat" wavelet basis in the density functional calculations. Now, we describe briefly how the wave functions are expressed in the Daubechies basis. Though a more complete description can be found in [17]. Both functions are localized, with compact support. All the properties of these functions can be obtained from the relations – see Fig.2:

$$\varphi(x)=\sqrt{2}\sum_{j=1-L}^{L}h_j\varphi(2x-j),\ \psi(x)=\sqrt{2}\sum_{j=1-L}^{L}g_j\psi(2x-j) \tag{13}$$

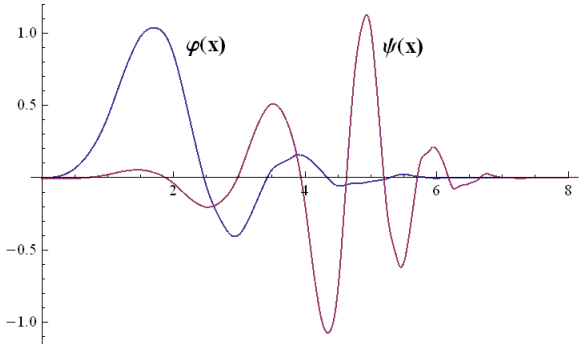

Figure 2. Scaling function φ(x) and wavelet function ψ(x) for L=6.

which relate the basis functions on a grid with spacing h and another one with spacing $h/2$. h_j and $g_j = (-1)^j h_{-j+1}$ are the elements of a filter that characterizes the wavelet family, and L is the order of the family. L=6 is the lowest number for which the wavelets and scaling functions possess the continuous first derivative, whereas L=10 – the second derivative. From Eq. (13), every scaling function and wavelet on a coarse grid of spacing Δz can be expressed as a linear combination of scaling functions at the finer grid level $\Delta z/2$. For this reason, wavelet functions complete the information which is lacking for refining the resolution level.
The function Z(z) can be approximated by scaling function φ(τ) at an arbitrary scale as:

$$Z(z)=\sum_{l=1}C_l\varphi(\tau-l),\quad z=\tau\Delta z,\ \tau=0,1,2,\ldots,n-1 \tag{14}$$

where the function is discretized at n points in the interval $[z_0,z_1]$. The detailed discussion of those problems is presented by Genovese et al. [19].
In the relations (11)-(14) the symbol C_l denotes the approximation coefficients.

4. Solution of the problem

In the present analysis the electron effective mass m_i is assumed to be constant on the quantum dot and the matrix for every fixed energy level E and is taken as [10]:

$$\frac{1}{m_i(E)} = \frac{P_i^2}{\hbar^2}\left(\frac{2}{E+E_{g,i}-V_i} + \frac{1}{E+E_{g,i}-V_i+\delta_i}\right) \tag{15}$$

where the confinement potential V_i is piecewise constant, and P_i , $E_{g,i}$ and δ_i are the momentum matrix element, the band gap, and the spin–orbit splitting in the valence band for the quantum dot ($i = q$) and the matrix ($2 = m$), respectively. The values of the above constants are given in Table 1.

	P_i	$E_{g,i}$	V_i	δ_i
i=1 (q) InAs	0.8503	0.42	0	0.48
i=2 (m) GaAs	0.8878	1.52	0.7	0.34

Table 1. The material properties of the quantum dot InAs and the matrix GaAs.

With the use of the relation (15) it is possible to use the identical approximations of the wave functions in the equations (3) and (4), since the different properties of the QD and the matrix are hidden in Table 1.
Using the properties of the Bessel function the numerator in the equation (3) takes the form eq. (16) whereas the denominator eq. (17).

$$a(\Phi,\Phi) = \sum_{i=1}^{2}\left(\frac{\hbar^2}{2m_i}D_1 + V_i D_2\right) \tag{16}$$

$$D_2 = \frac{r_0^2 dz}{2}F(A_m)\sum_{n=0}^{\infty}\left[\frac{n\pi}{z_1-z_0}C_n\right]^2,\ D_1 = -dz\sum_{n=0}^{\infty}[C_n]^2\sum_{m,k=0}^{\infty}A_m A_k\frac{\mu_m^{(l)}\mu_k^{(l)}}{r_0^2}\int_0^{r_0}drJ_{l-1}\left(\frac{\mu_k^{(l)}r}{r_0}\right)J_{l+1}\left(\frac{\mu_m^{(l)}r}{r_0}\right)$$

$$b(\Phi,\Phi) = \frac{r_0^2 dz}{2}F(A_m)\sum_{n=0}^{\infty}[C_n]^2,\ F(A_m) = \sum_{m=0}^{\infty}\left[A_m J_l'\left(\mu_m^{(l)}\right)\right]^2,\ dz = \frac{z_1 - z_0}{2} \tag{17}$$

The computation is carried out in the iterative way in two steps:

1. For the assumed value of the eigenenergy E_0 the minimum of the functional $a(\Phi,\Phi)$-$E_0 b(\Phi,\Phi)$ is searched for, with respect to the unknown coefficients A_m and C_n,
2. For the calculated values of A_m and C_n a rational matrix eigenvalue problem (4) is solved to determine a new eigenvalue E_1.

The procedure is repeated until the required accuracy is reached. The computations are conducted with the use of the symbolic package Mathematica.

5. Performance Results

We have applied our method on two different problems in order to test its efficiency and effectiveness. Figure 3 demonstrates the axisymmetrical conical quantum dot embedded in the axisymmetric cylindrical matrix. The radius and the height of the QD are equal to 10, whereas the radius and the height of the matrix are equal to 40 and 30, respectively. The physical

properties of the materials are given in Table 1. The boundary conditions are assumed to be in the Dirichlet form, i.e. the wave functions are equal to zero on the boundaries.

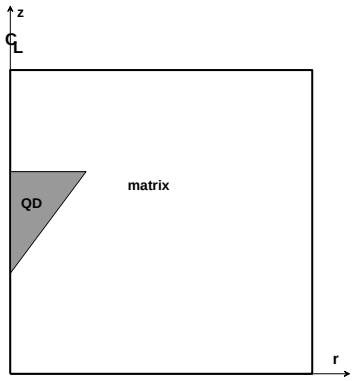

Figure 3. Geometry of the quantum dot surrounded by the matrix

Table 2 shows the results of the computations. The results are presented for the first six eigenvalues and compared also with the results available in the open literature.

The electron orbital quantum number	Eigenvalue- present analysis			Eigenvalue-Voss [5] Finite element (planar) 6000
	Fourier expansion 15 to 20 terms	Finite element 30 (linear)	Wavelet L=12	
0	0.254607	0.255243	0.258931	0.254585
1	0.387332	0.386121	0.395571	0.384162
0	0.466941	0.469542	0.471121	0.467239
2	0.502889	0.503891	0.504005	0.503847
0	0.560774	0.562781	0.564451	0.561319
1	0.599138	0.604511	0.597138	0.598963
3	0.622213	0.634115	0.623356	0.617759

Table 2. Eigenvalues for the conical quantum dot embedded in the matrix

The computed eigenvalues shows quite good agreement with the results obtained by Voss [5]. In present the computations the maximal number of terms in the expansions of the function Z(z) is different, however, the use of the linear finite element or the wavelet approximations seems to be much more reasonable that the application of the finite element discretization with the use of the triangular elements. The approximation in the radial direction (10) was cut off on the maximal 50 terms. It is worth to note that the lowest values of the eigenvalues do not correspond to the lowest values of the electron orbital quantum number.
The next example deals with the analysis of the pyramidal quantum dots (with slightly rounded corners due to the use of the approximation (7)) embedded in the cuboidal (with rounded corners) matrix. The results are given in Table 3.

The electron orbital quantum number	Eigenvalue- present analysis			Eigenvalue-Voss [5] Finite element (tetrahedrons) 6000
	Fourier expansion 15 to 20 terms	Finite element 30 (linear)	Wavelet L=12	
0	0.254607	0.255243	0.258931	0.254585
1	0.387332	0.386121	0.395571	0.384162
0	0.466941	0.469542	0.471121	0.467239
2	0.502889	0.503891	0.504005	0.503847
0	0.560774	0.562781	0.564451	0.561319
1	0.599138	0.604511	0.597138	0.598963
3	0.622213	0.634115	0.623356	0.617759

Table 3. Eigenvalues for the pyramidal quantum dot embedded in the matrix

6. Concluding Remarks

The present method shows the possibility of analytical computations of nonlinear boundary value problem characterized by the Helmholtz equations. In this way it is possible to find not only the energy spectrum and wave functions of an electron in a quantum dot but also the acoustic eigenfrequencies and eigenmodes of the pressure field inside an acoustic cavity. Eigensolutions are presented in the convenient form of the series expansions. The analysis can be conducted for the arbitrary form of the potential function, however having the axisymmetry with respect to the axis of rotations.

REFERENCES

[1] M. Grundmann, O. Stier, and D. Bimberg, *Phys. Rev. B* **52**, 11969 (1995).
[2] O. Stier, M. Grundmann, and D. Bimberg, *Phys. Rev. B* **59**, 5688 (1999).
[3] H.T. Johnson, L.B. Freund, The influence of strain on confined electronic states in semiconductor quantum structures, *Int. J. Sol. Struct.* **38** ,1045-1062 (2001).
[4] F. Gelbard and K. J. Malloy , Modeling Quantum Structures with the Boundary Element Method, *J. Comp. Phys.* **172,** 19–39 (2001).
[5] H. Voss, Numerical calculation of the electronic structure for three-dimensional quantum dots, *Comp. Phys. Communications* **174**, 441-446 (2006).
[6] L.C. Lew Yan Voon, M. Willatzen, Helmholtz equation in parabolic rotational coordinates: application to wave problems in quantum mechanics and acoustics, *Math. Comp. in Simulation* **65**, 337–349, (2004).
[7] M. Willatzen, L.C. Lew Yan Voon, Numerical implementation of the ellipsoidal wave equation and application to ellipsoidal quantum dots, *Comp. Phys. Communications* **171**, 1–18, (2005).
[8] Y. Li, An iterative method for single and vertically stacked semiconductor quantum dots simulation, *Math. Comp. Modelling* **42**, 711-718, (2005).
[9] G. Cattapan, P.Lotti, A.Pascolini, A scattering-matrix approach to the eigenenergies of quantum dots, *Physica E* **41**,1187-1192, (2009).
[10] Zaslavsky, A., Milkove, K.R., Lee, Y.H., Ferland, B., Sedgewick, T.O., 1995. Strain relaxation in silicon/germanium microstructures observed by resonant tunneling spectroscopy. Applied Physics Letters 67, 3921.
[11] Pan E. Elastic and piezoelectric fields around a quantum dot: fully coupled or semicoupled model, J Appl Phys 2002;91(6):3785–96.
[12] Jogai B, Albrecht JD, Pan E. Effect of electromechanical coupling on the strain in AlGaN/GaN HFETs. J Appl Phys 2003;94:3984–9.
[13] Melnik R., Mahapatra R., Coupled effects in quantum dot nanostructures with nonlinear strain and bridging modelling scales, Computers and Structures 85 (2007) 698–711
[14] Muc A., An analytical solution for conical quantum dots, J. Theor Appl Mech. (to be published in 2013).
[15] Boyer CP., E. G. Kalnins E.G., Miller W., Jr., Symmetry and Separation of Variables for the Helmholtz and Laplace Equations, Nagoya Math. J. , 60 (1976), 35-80
[16] G. Strang, G.J. Fix, An Analysis of the Finite Element Method, Wellesley-Cambridge Press, 1988.
[17] Cho K., Arias T.A., Joannopolous J.D., Lam P.K, Wavelets in Electronic Structure Calculations, Phys. Rev. Letters 71 (1993) 1808-1811.
[18] I. Daubechies, Ten Lectures on Wavelets, SIAM, Philadelphia, 1992.